Preparation and characterization of in-plane polarized PZT piezoelectric diaphragms

Yi Yin (尹 伊)*, Kangcheng Qi (祁康成), Zhicai Xu (许志财), Yugong Zeng (曾愈巩), and Zulun Lin (林祖伦)

School of Optoelectronic Information, University of Electronic Science and Technology of China, Chengdu 610054, China

**Corresponding author: yinyi@uestc.edu.cn*

Received January 4, 2013; accepted January 26, 2013; posted online June 14, 2013

The preparation and characterization of in-plane polarized lead zirconate titanate (PZT) piezoelectric diaphragms for sensors and actuators applications are demonstrated in this letter. The single phase PZT films can be obtained on SiO_2-passivated silicon substrates via sol-gel technique, in which $PbTiO_3$ (PT) films are used as seed layers. Al reflective layer is deposited and patterned into concentric interdigitated top electrode by lithographic process, subsequently. The diaphragms are released using orientation-dependent wet etching (ODE) method. The size of the diaphragms is 5 mm in diameter and the outer interdigitated (IDT) electrode diameter (4.25 mm) is fixed at 85% of the diaphragm diameter. The three-dimensional (3D) profiles results indicate that the measured maximum central deflection at 15 V is approximately 9 μm. Sensing measurements show that the capacitance continually decreases with an increase of applied force, while the case of induced charge exhibits a reverse tendency.

OCIS codes: 160.2260, 160.6060, 220.1080, 220.4000.

doi: 10.3788/COL201311.S10403.

Because of the advantages of perfect piezoelectric activity, low inertia, and relatively small size, lead zirconate titanate (PZT) thin films have been intensively applied in various microelectromechanical (MEMS) actuators and sensors such as adaptive optical (AO) device, pressure and acoustic transducers, and accelerometers[1−5]. At present, many designs for piezoelectric MEMS devices utilize the bending of cantilever or diaphragm structures[6]. Typically a bending unit consists of a piezoelectric layer sandwiched between two metal electrodes and supported on a passive layer (and so, poled through the thickness, called d_{31} mode)[7,8]. The basic idea of such configuration is to transfer the transverse piezoelectric strain to a large bending deformation in the perpendicular direction. Mechanical bending of the configuration can greatly amplify the deformation caused by the PZT films for actuator applications or the applied stress on the PZT films for sensor applications. It should be noticed that, in perovskite ferroelectrics, the d_{33} piezoelectric constant is often twice of the d_{31} constant[9], so considerable improvements can be expected for d_{33}-mode piezoelectric devices compared to d_{31}-mode ones. Furthermore, concentric interdigitated (IDT) electrode configurations, one-dimensional (1D) without bottom electrodes, are the easiest way to realize the d_{33} piezoelectric coupling via silicon micromachining technology. Compared with cantilever or bridge structures, concentric IDT electrodes with diaphragm structures, where the PZT films are polarized in the film plane rather than through the thickness, can utilize both d_{31} and d_{33} effect. This configuration also possesses the advantage of decoupling the device capacitance from the thickness. In order to achieve this aim, PZT films were successfully deposited on SiO_2-passivated silicon substrates and shown to possess excellent in-plane polarization[10]. Meanwhile, a thin $PbTiO_3$ (PT) buffer layer was interposed to improve the crystallinity of PZT layer[11]. In this letter, the actuating and sensing characteristics of such in-plane polarized PZT films are estimated and compared to the conventional PZT films polarized in thickness direction.

Experimentally, the PZT sols were prepared by using lead acetate trihydrate ($Pb(CH_3COO)_2{\cdot}3H_2O$, 99.5%, analytical pure), tetrabutyl titanate ($(C_4H_9O)_4Ti$, 98.5%, analytical pure), and zirconium n-propoxide ($Zr(OC_3H_7)_4$, 15% in n-propoxide, Aldrich) as raw materials. All of them were diluted by 2-methoxyethanol ($CH_3OC_2H_4OH$, 99.0%, analytical pure). The components of PZT and PT precursor solutions, with the same molarities of 0.1 mol/L, were controlled in the ratios of Pb:Zr:Ti=1.1:0.52:0.48 and Pb:Ti=1.06:1. The respective 10% and 6% Pb in excess of stoichiometry could compensate for high Pb volatility during heat treatment. Acetylacetone (20 vol%) and acetic acid (5 vol%) were selected as an additive to adjust the solution viscosity and stability in order to reduce the risk of cracks on PZT thin films. All of the experimental processes were carried in a dry argon atmosphere to inhibit the moisture. PT buffer layer and PZT film, 1 and 20 layers respectively, were deposited on Si substrates ((100), polished on one side) with 1-μm SiO_2 thermal oxide by using spin-coating and layer-by-layer annealing method. Then, Al electrodes were evaporated on the top surface of PZT thin films and patterned into concentric IDT electrodes via standard photolithography. The IDT electrodes, as shown in Fig. 1, were defined with a finger width of 100 μm and a finger gap (electrode spacings) of 20 μm, respectively. Finally, the diaphragms were released via orientation-dependent wet etching (ODE) method[12]. To meet the mechanical stability, the residual silicon layer was kept to 5–10 μm for actuating and sensing measurement. The detailed method of preparation can be found in our former reports[10].

The crystallinity of PZT film was analyzed by the X-ray diffractometer (D/MAX, R-A) with a

 © 2013 Chinese Optics Letters

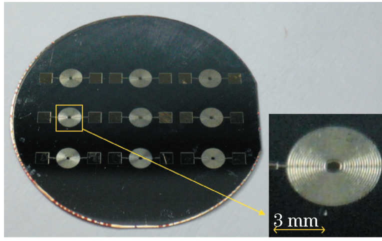

Fig. 1. Photographs of the fabricated IDT electrode patterns.

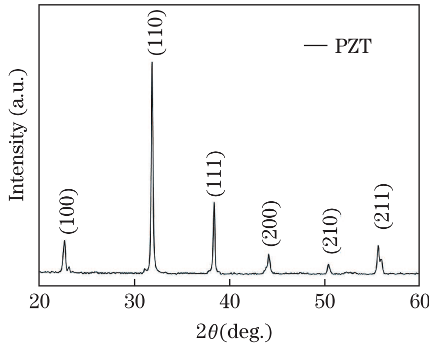

Fig. 2. XRD pattern of the PZT film.

copper target, at 40 kV, 40 mA. The results are shown in Fig. 2, in which the PZT film exhibits a pure perovskite phase. Formation of the unwanted pyrochlore phase was eliminated through a careful selection of deposition parameters. The peak with the highest intensity in the X-ray diffraction (XRD) pattern of the PZT film is indexed as the (101) plane, indicating that the films deposited were polycrystalline in nature which is similar to the bulk PZT ceramic. This is because a polycrystalline system provides for alleviation of stress through relaxation mechanisms. The surface and cross-sectional microstructures of the films were observed using atomic force microscope (AFM, ZJU-II, ZJU) and field emission scanning electron microscopy (SEM, FEI, SIRON), respectively. The results are shown in Fig. 3. The AFM micrograph (Fig. 3(a)) of the PZT film suggests a grain aggregate structure in 1–5 mm scale, but actual grain size is relatively smaller because of the integration effect. The SEM image (Fig. 3(b)) shows the clear multilayer PZT, SiO_2, Si structures and very sharp interfaces between the PZT and SiO_2 films. The thicknesses of the PZT and SiO_2 layers are approximately 830 and 240 nm, respectively. Moreover, its structure is crack-free and uniform, which do not fracture to reveal individual layers (including the PT layer). These observations suggest that the adhesion between each sublayer of the PZT film is very good and the passivated SiO_2 can work as an effective buffer layer preventing the reaction and interdiffusion between the PZT film and silicon substrate.

The static actuating capability of PZT diaphragm can be estimated by the bending displacement in the perpendicular direction. Therefore, in this letter, the deformation measurements of the diaphragm were carried out via an interferometric profiler (Zygo, PTI-250). It is also important to note that, before these measurements, the PZT film should be poled at 150 kV/cm (∼three times as much as the coercive fields of PZT films)[13] for 20 min at 200 °C in order to align the ferroelectric domains in polar direction. The deflection profiles of the diaphragm under different applied voltages were shown in Fig. 4. The results indicated that the diaphragm can generate 2–9 μm deflections with low operating voltages, which can compare with that reported by other teams[14,15], but the deformation behaviors exhibit different outline-change trend with the applied electric field, presumably due to the reaction between residual stress and converse piezoelectric effect of PZT films. The detailed intrinsic strain behaviors of the diaphragm can be evaluated via finite element method (FEM)[16].

The sensing performance of the PZT diaphragm was characterized via the modified wafer flexure platform[17], as shown in Fig. 5. The sample was firstly fastened over a cylinder cavity to form a closed system. Then, the air pressure in the cavity was modulated via the vacuum pump and the digital pressure transducer. The PZT diaphragm was flexed periodically with the output of an audio speaker under different voltages. A biaxial, transverse stress was then generated in the diaphragm, and hence, a piezoelectrically induced charge can be detected by the peripheral amplifier circuit. Meanwhile, the film capacitance as a function of applied voltage was also carried out via semiconductor parameter analyzer (Agilent, 4511c).

Figure 6 shows the capacitances and induced charge values of the in-plane polarized diaphragm with various pressure oscillation levels. The results suggest a successive decrease of capacitance with the pulse signal amplitudes from 5 to 20 V, but an obvious reverse tendency of the induced charge changes with the pulse signal amplitudes from 5 to 20 V. In addition, the reduction of film

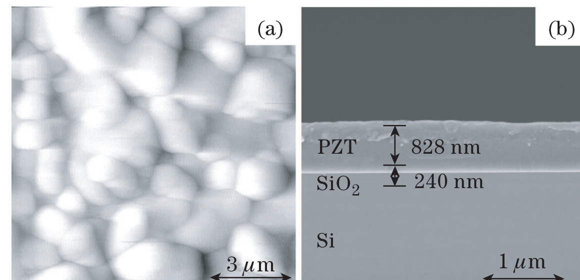

Fig. 3. (a) AFM results of surface microstructure of the PZT film; (b) SEM results of cross-sectional microstructure.

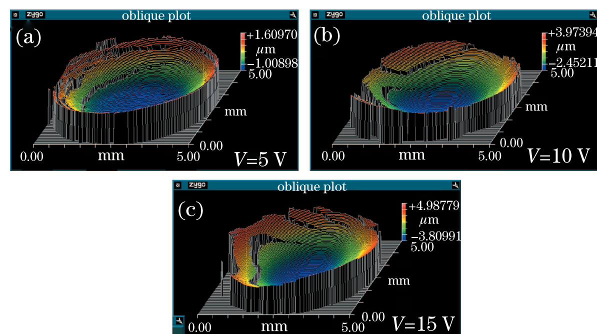

Fig. 4. (Color online) Three-dimensional (3D) deflection profiles of PZT diaphragm under (a) 5, (b) 10, and (c) 15 V.

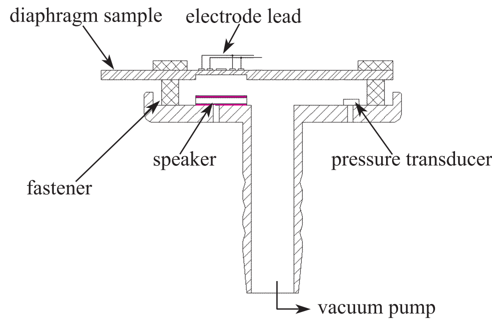

Fig. 5. Sketch of sensing measurement setup.

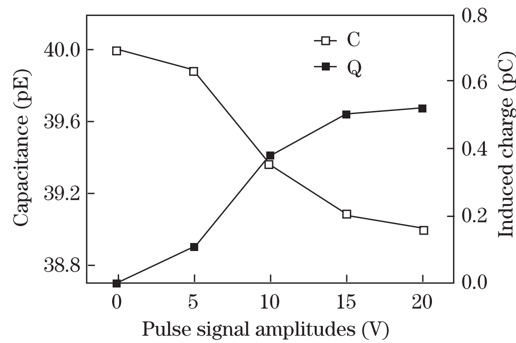

Fig. 6. Film capacitance and induced charge of in-plane polarized PZT film with various pressure oscillation levels.

capacitance with the pulse signal amplitudes from 5 to 10 V is larger than the decrease of capacitance during the range of 10–20 V. The similar phenomenon can also be seen in the change of induced charge with the pulse signal amplitudes, which may attribute to the same reason that the deflection of PZT diaphragm reaches a saturation value near pulse signal amplitude V=20 V.

In conclusion, the actuating and sensing characteristics of in-plane polarized PZT piezoelectric diaphragms are demonstrated in this letter. PT and PZT films are prepared by the similar sol-gel process on SiO_2-passivated silicon substrates. The SiO_2 barrier layer can effectively inhibit interdiffusion while the PT layer can improve the crystallinity of PZT film. The diaphragms are released via ODE method. Because the concentric IDT can couple d_{31} and d_{33} piezoelectric effect, for diaphragms configurations, larger deflection can be obtained under low driving voltage. The results indicate that the measured maximum central deflection at 15 V is approximately 9 μm, which is larger than that of the conventional, parallel-plate actuators. The sensing measurement shows the capacitance continually decreases with an increase of applied force, while the case of induced charge exhibits a reverse tendency. Thus, further work can be expected to construct devices such as deformable mirror for AO systems and diaphragm sensors for underwater acoustics via the in-plane polarized PZT diaphragms through developed MEMS technology.

This work was supported by the Fundamental Research Funds for the Central Universities under Grant No. ZYGX2012J059.

References

1. J. A. Perreault, T. G. Bifano, B. M. Levine, and M. N. Horenstein, Opt. Eng. **41,** 561 (2002).
2. D. L. Polla and L. F. Francis, MRS Bull. **21,** 59 (1996).
3. Z. H. Wang, J. M. Miao, and C. W. Tan, Sens. Actuators A **54,** 530 (1996).
4. C. Lee, T. Itoh, and T. Suga, IEEE Trans. Ultrason. Ferroelectr. Freq. Control **43,** 553 (1996).
5. L. E. Cross and S. Trolier-McKinstry, Encl. Appl. Phys. **21,** 429 (1997).
6. R. Maeda, J. J. Tsaur, S. H. Lee, and M. Ichiki, J. Electroceramics. **12,** 89 (2004).
7. H. Kueppers, T. Leuerer, U. Schnakenberg, W. Mokwa, M. Hoffmann, T. Schneller, U. Boettger, and R. Waser, Sens. Actuators A **97-98,** 680 (2002).
8. Y. Hishinuma and E. H. Yang, J. Microelectromech. Syst. **15,** 686 (2006).
9. A. J. Moulson and J. M. Herbert, *Electroceramics* (Chapman & Hall, London, 1990).
10. Y. Yin, H. Ye, W. B. Zhan, L. Hong, H. M. Ma, and J. Xu, Sens. Actuators A **171,** 332 (2011).
11. S. K. Pandeya, A. R. Jamesa, C. Prakasha, T. C. Goelb, and K. Zimikc, Mater. Sci. Eng. B **112,** 96 (2004).
12. K. R. Williams and R. S. Muller, J. Microelectromech. Syst. **5,** 256 (1996).
13. R. A. Wolf and S. Trolier-McKinstry, J. Appl. Phys. **95,** 1397 (2004).
14. C. Zinck, D. Pinceau, E. Defay, E. Delevoye, and D. Barbier, Sens. Actuators A **115,** 483 (2004).
15. E. Hong, S. V. Krishnaswamy, C. B. Freidhoff, and S. Trolier-McKinstry, Sens. Actuators. A **119,** 520 (2005).
16. E. Hong, S. Trolier-McKinstry, R. L. Smith, S. V. Krishnaswamy, and C. B. Freidhoff, J. Microelectromech. Syst. **15,** 832 (2006).
17. J. F. Shepard Jr., P. J. Moses, and S. Trolier-McKinstry, Sens. Actuators A **71,** 133 (1998).